

## High power Silicon laser based on the dressed photon technology

Tadashi Kawazoe

Tokyo Denki University.

Tokyo Senju Campus, Bldg.4-9F 906A

5 Senju-Asahi-cho, Adachi-kuChiyoda-ku, Tokyo 120-8551, Japan

Phone: +81-3-5284-5981 E-mail: kawazoe@mail.dendai.ac.jp

### Abstract

**A Silicon laser based on the dressed photon technology is reviewed. A dressed photon generated at around a dopant-atom pair is easily coupled with phonon which is satisfied the conservation law of wavenumber for the radiative recombination of Silicon. The silicon laser operates via the dressed photon state couple with phonons.**

### 1. Introduction

Radiative recombination life time of electrons and holes in the indirect-transition-type semiconductor is very long. Due to this physical property, usually, indirect-transition-type semiconductors including with Silicon (Si) are not suitable materials for light-emitting devices, for example, light emitting diode (LED), a laser diode (LD), and so on. In spite of this disadvantage, the light emitters using Si have been studied due to many other advantages, for example, compatibility with electronics, low-cost, an abundant supply, and so on[1-3]. The realization of Si laser also has been studied. In recent years, Si Raman lasers [2] and a stimulated emission of a Si quantum wells are reported. In these previous studies, the physical mechanisms are based on a conventional semiclassical solid-state physics of optical properties.

We have also reported a unique radiative recombination mechanism in the indirect-transition-type semiconductor based on the dressed photon and Si laser has been also developed by using this mechanism [5,6]. We have achieved the laser output power of more than 10 W so far. In the presentation, I review the dressed-photon-phonon annealing for fabrication of the light-emittable Si pn junction, first. Second, we demonstrate current injection type high power Si laser with a unique design. Its lasing threshold current density decreased to 60A/cm<sup>2</sup> and the output power of the laser increased to 13W at the wavelength of 1.34μm for the current density of 100A/cm<sup>2</sup>. Finally, I demonstrate Si lasers with the reflection layers fabricated at the both end of the laser chip. Its threshold current was decreased to 40% (the current density of 22 A/cm<sup>2</sup>). The lasing wavelength was 1190 nm due to the spectral properties of the reflection layers.

### 2. DPP annealing and Dressed-Photon-Phonon Emission

The fabrication methods of the Si light emitting device with the p-n junction have already reported [7-13]. First, the p-n homojunction was fabricated by the ion-implanting of a p-dopant (Boron:B) into an n-type Si substrate which was As-doped n-type Si wafer with an electrical resistivity of 10

Ω•cm. The energy of the ion-implantation for the B doping was 700 keV, and the dose density was 5×10<sup>13</sup> cm<sup>-2</sup>. Second, in order to optical activation of the Si p-n junction, the fabricated p-n homojunction is annealed by Joule heating causing the forward injection current. During this annealing process, the p-n homojunction is irradiated by the infrared light. This annealing process has been named DPP (dressed photon-phonon) annealing.

The dressed photon-phonon (DPP) is a quasi-particle formed by the coupling of photon and phonon via an electron-hole pair in the materials [14]. For creation of DPP, the dopant pair is very important. Generally, the interaction between a photon and a phonon is more than 10<sup>-3</sup> smaller than that between a photon and electron, which is nearly equal to the mass ratio between an electron and a nucleus. Beside, when B dopant pair in the Si crystal acts as the confinement boundaries for phonons causing the difference of mass between Si and B atoms, the phonon density drastically increases, which is satisfying confinement boundary condition. In the previously theoretical calculation [14], the phonon density in the B dopant pair becomes more than 10<sup>4</sup> times higher than that in the pure Si crystal. In the experiment, the Huang-Rhys factor of 4.08 using DPP annealed Si p-n junction, giving the coupling strength between electrons and optical mode phonons has been obtained [13]. This value is 10<sup>3</sup> times larger than that in bulk Si crystals. Thus, if B dopant pair in the Si crystal well acts as the confinement boundaries for phonons, the total interaction strength between a photon and a phonon become as same as that between a photon and an electron. When the wavenumber of a confined phonon in B pair is equal to the wavenumber difference between an electron at the bottom in the conduction band and a hole at the top in the valence band of a Si crystal, the radiative recombination rate increases and the radiation efficiency of the Si becomes as same as the direct transition type semiconductors..

### 3. 10W Si laser

An Sb-doped n-type Si wafer with an As-doped n-type epitaxially formed layer was used as a device substrate. The thickness and the electrical resistivity were 10 μm and 10 Ω•cm, respectively. Boron (B) was induced in this epitaxial layer as a p type dopant by ion implantation. The implantation energy and dose density were 700 keV and 5×10<sup>13</sup> cm<sup>-2</sup>, respectively. After the implantation, the external shape of the laser cavity was formed by a polishing and a cleaving. The size of the cavity was 15 mm × 1 mm × 150 μm (length × width × thickness).

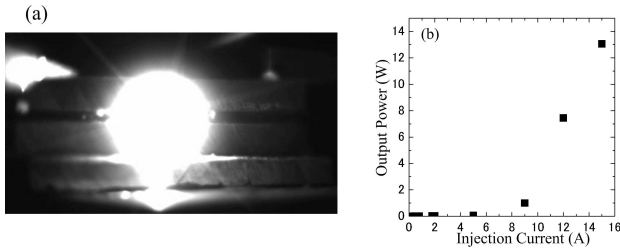


**Fig1.** (a) infrared photograph of the operating Si laser. (b) The injection current dependence of the laser output power.

Figure 1(a) shows the photograph of the front view of the Si laser device in operation taken by the infrared camera. Figure 1(b) shows a injection current dependence of the laser output power. Its lasing threshold current density decreased to  $60\text{A}/\text{cm}^2$  and the output power of the laser increased to  $13\text{W}$  at the wavelength of  $1.34\mu\text{m}$  for the current density of  $100\text{A}/\text{cm}^2$ . The obtained threshold current density is very low comparing with the conventional semiconductor lasers and the output power was more than  $10^5$  times larger than previous Si lasers that we fabricated. The lasing spectral line width was more than  $100\text{ nm}$ , because the device was a multimode broad area laser. The external power efficiency was about  $20\%$ , and the external quantum efficiency was  $80\%$ . We consider the high quantum efficiency comes from the multi-step transition via dressed-photon state.

#### 4. Si Laser with Reflective layers

After deposition of a gold (Au) film as electrodes, the reflective coating layers were deposited on both end-side of the Si laser cavity. Finally, the laser chip was mounted on the Copper mounting plate. After the mounting, the laser device was DPP-annealed. Here, we used the annealing laser with a wavelength of  $1342\text{ nm}$  and a power of  $4\text{W}$ . The applying a forward-bias current was  $4.5\text{ A}$ .

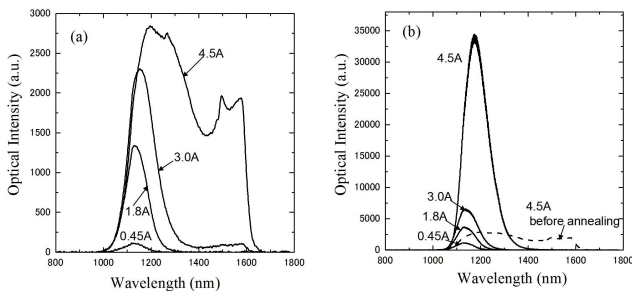


**Fig.2.** Emission spectra from the Si lasers (a) before DPP annealing (b) after DPP annealing.

Figure 2 (a) shows EL spectra from the Si laser chip for the currents of  $0.45\text{ A}$ ,  $1.8\text{A}$ ,  $3.0\text{A}$ , and  $4.5\text{A}$  before DPP annealing. The spectral peak appeared at the wavelength of  $1140\text{nm}$  corresponds to the Si indirect band gap energy for the lower current and it shifted to longer wavelength with the increase in the injection current. Additionally, another emission band appeared in the wavelength region of  $1400\text{-}1600\text{ nm}$ . The solid curves in Fig.2(b) show EL spectra from the Si laser chip for the currents of  $0.45\text{ A}$ ,  $1.8\text{A}$ ,  $3.0\text{A}$ , and  $4.5\text{A}$  after DPP annealing. The peak emission wavelength appeared at  $1180\text{ nm}$ . The emission intensity increased and single emission peak appeared. The

broken curve in Fig.2 (b) shows a emission spectrum before DPP annealing for the injection current of  $4.5\text{ A}$ . The spectra for injection current of  $4.5\text{ A}$  had fine oscillatory structures. We consider this structure indicates the lasing of the Si chip.

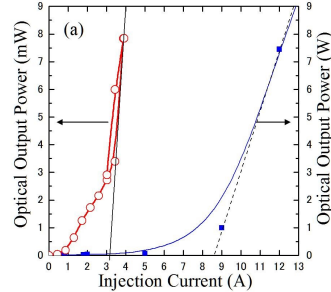


**Fig.3.** Optical output power VS Injection current.

Figure 3 shows a current dependency of output optical power from the Si laser chip with the reflection layer (open circles) and without reflection layer (closed squares). The laser oscillation threshold current of the fabricated Si laser with the reflection layers was  $3.3\text{ A}$ , which corresponds to the current density of  $22\text{ A}/\text{cm}^2$ . This is about  $40\%$  for the threshold current of Si laser without reflection layers.

#### 5. Conclusions

I have explained the dressed-photon-phonon annealing for fabrication of the light-emittable Si pn junction. We demonstrate current injection type high power Si laser with a unique design. Its lasing threshold current density decreased to  $60\text{A}/\text{cm}^2$  and the output power of the laser increased to  $13\text{W}$  at the wavelength of  $1.34\mu\text{m}$  for the current density of  $100\text{A}/\text{cm}^2$ . Finally, I demonstrate Si lasers with the reflection layers fabricated at the both end of the laser chip. Its threshold current was decreased to  $40\%$  (he current density of  $22\text{ A}/\text{cm}^2$ ). The lasing wavelength was  $1190\text{ nm}$  due to the spectral properties of the reflection layers.

#### References

- [1]. D. Liang, and J. E. Bowers, *Nat. Photonics* **4**, 511 (2010).
- [2]. H. Rong, R. Jones, A. Liu, O. Cohen, D. Hak, A. Fang, and M. Paniccia, *Nature* **433**, 725 (2005).
- [3]. S. Saito, Y. Suwa, H. Arimoto, N. Sakuma, D. Hisamoto, H. Uchiyama, J. Yamamoto, T. Sakamizu, T. Mine, S. Kimura, T. Sugawara, and M. Aoki, *Appl. Phys. Lett.* **95**, 241101 (2009).
- [4]. Russell D Uptis, *IEEE J. Quant. Electron.* Vol. **23**, NO. 6, 651(1987). "An Introduction to the Development of the Semiconductor Laser"
- [5]. T. Kawazoe, M. Ohtsu, K. Akahane, N. Yamamoto, *Appl. Phys. B*, **107**, 659 (2012).
- [6]. H. Tanaka, T. Kawazoe, M. Ohtsu, K. Akahane, *Fluorescent Materials*. **1**, 1 (2015).
- [7]. T. Kawazoe, M. A. Mueed, M. Ohtsu, *Appl. Phys. B*, **104**, 747–54 (2011).
- [8]. N. Wada, T. Kawazoe, M. Ohtsu, *Appl. Phys. B*, **108**, 25–29 (2012).
- [9]. H. Tanaka, T. Kawazoe, M. Ohtsu, *Appl. Phys. B*, **108**, 51–56 (2012).
- [10]. M. A. Tran, T. Kawazoe, M. Ohtsu, *Appl. Phys. A*, **115**, 105–111(2014).
- [12]. N. Wada, M. A. Tran., T. Kawazoe, M. Ohtsu, *Appl. Phys. A*, **115**, 113–118 (2014).
- [13]. M. Yamaguchi, T. Kawazoe, M. Ohtsu, *Appl. Phys. A*, **115**, 119–125 (2014).
- [14]. Y. Tanaka, K. Kobayashi, *Physica E* **40**, 297 (2007).